

RESEARCH ARTICLE

10.1002/2015JG003185

Key Points:

- Soil crusts switch between reversing and promoting desertification
- Soil crusts were essential to reversal of land degradation in Lehavim LTER
- Results resolve divergent findings on effect of soil crusts on vegetation loss

Supporting Information:

- Supporting Information S1

Correspondence to:

S. Assouline,
vwshmue@agri.gov.il

Citation:

Assouline, S., S. E. Thompson, L. Chen, T. Svoray, S. Sela, and G. G. Katul (2015), The dual role of soil crusts in desertification, *J. Geophys. Res. Biogeosci.*, 120, 2108–2119, doi:10.1002/2015JG003185.

Received 17 AUG 2015

Accepted 1 OCT 2015

Accepted article online 11 OCT 2015

Published online 30 OCT 2015

The dual role of soil crusts in desertification

S. Assouline¹, S. E. Thompson², L. Chen³, T. Svoray⁴, S. Sela⁴, and G. G. Katul^{5,6}
¹Institute of Soil, Water and Environmental Sciences, A.R.O., Volcani Center, Bet Dagan, Israel, ²Department of Civil and Environmental Engineering, University of California, Berkeley, California, USA, ³Division of Hydrologic Sciences, Desert Research Institute, Las Vegas, Nevada, USA, ⁴Geography and Environmental Development, Ben-Gurion University of the Negev, Beer Sheva, Israel, ⁵Nicholas School of the Environment, Duke University, Durham, North Carolina, USA, ⁶Pratt School of Engineering, Duke University, Durham, North Carolina, USA

Abstract Vegetation cover in dry regions is a key variable in determining desertification. Soils exposed to rainfall by desertification can form physical crusts that reduce infiltration, exacerbating water stress on the remaining vegetation. Paradoxically, field studies show that crust removal is associated with plant mortality in desert systems, while artificial biological crusts can improve plant regeneration. Here it is shown how physical crusts can act as either drivers of or buffers against desertification depending on their environmental context. The behavior of crusts is first explored using a simplified theory for water movement on a uniform, partly vegetated slope subject to stationary hydrologic conditions. Numerical model runs supplemented with field data from a semiarid Long-Term Ecological Research site are then applied to represent more realistic environmental conditions. When vegetation cover is significant, crusts can drive desertification, but this process is potentially self-limiting. For low vegetation cover, crusts mitigate against desertification by providing water subsidy to plant communities through a runoff-runon mechanism.

1. Introduction

Desertification poses a threat to the productivity of global drylands—a region that covers some 40% of Earth's land surface and houses 40% of the world population [D'Odorico *et al.*, 2013; *Millennium Ecosystem Assessment*, 2003; Reynolds *et al.*, 2007; Scheffer *et al.*, 2001; United Nations, 1994]. Although climatic variation, particularly drought, is associated with desertification, human management of drylands, including clearing, agriculture, grazing, and restoration activities often represent the ultimate causes of desertification, typically through their impacts on soil changes and erosion [Barbero-Sierra *et al.*, 2015; Miao *et al.*, 2015; Torres *et al.*, 2015; Wang *et al.*, 2013]. The global economic and social pressures that influence human management of drylands are rapidly changing, creating an urgent need to understand options for improving drylands management [Bisaro *et al.*, 2014; Fleskens and Stringer, 2014]. In this context, this study attempts to clarify an ongoing point of contention in drylands research: namely, whether the formation of physical soil crusts, widely associated with desertification, primarily enhances or diminishes the water available to vegetation, and thus the trajectory of plant cover in drylands.

Desertification is broadly defined as “land degradation in arid, semiarid, and dry subhumid areas,” meaning that a wide suite of physical, economic, and social processes can be said to contribute to desertification [United Nations Convention to Combat Desertification, 2012]. Indeed, determining whether a landscape is undergoing desertification remains an active area of research, discussion, and contention [Bisaro *et al.*, 2014; Salvati *et al.*, 2013]. Landscapes can become degraded through changes in vegetation diversity and productivity [Álvarez-Martínez *et al.*, 2013; Kröpl *et al.*, 2013], and simple measures of landscape greenness or fractional vegetation cover are challenging to interpret in terms of the overall health of arid landscapes (e.g., the recent greening trend in the Sahel has been variously interpreted as due to increasing woody vegetation cover [Brandt *et al.*, 2015], increasing herbaceous cover [Dardel *et al.*, 2014], and as the result of a complex interaction of climate and land management trends [Olsson *et al.*, 2005]). Nonetheless, the majority of degradation processes in arid landscapes induce a decline in vegetation fractional cover [Deblauwe *et al.*, 2008; Schlesinger *et al.*, 1990; Vicente-Serrano *et al.*, 2012] and an expansion of bare soil areas. The ecohydrological effects of these bare soil areas in terms of their impacts on plant available water (the major limiting factor for plant growth in arid environments) determine whether degradation processes are amplified or dampened by initial declines in vegetation cover. The interplay between fractional vegetation cover and plant available water, as mediated by soil and runoff processes, forms the focus of this study.

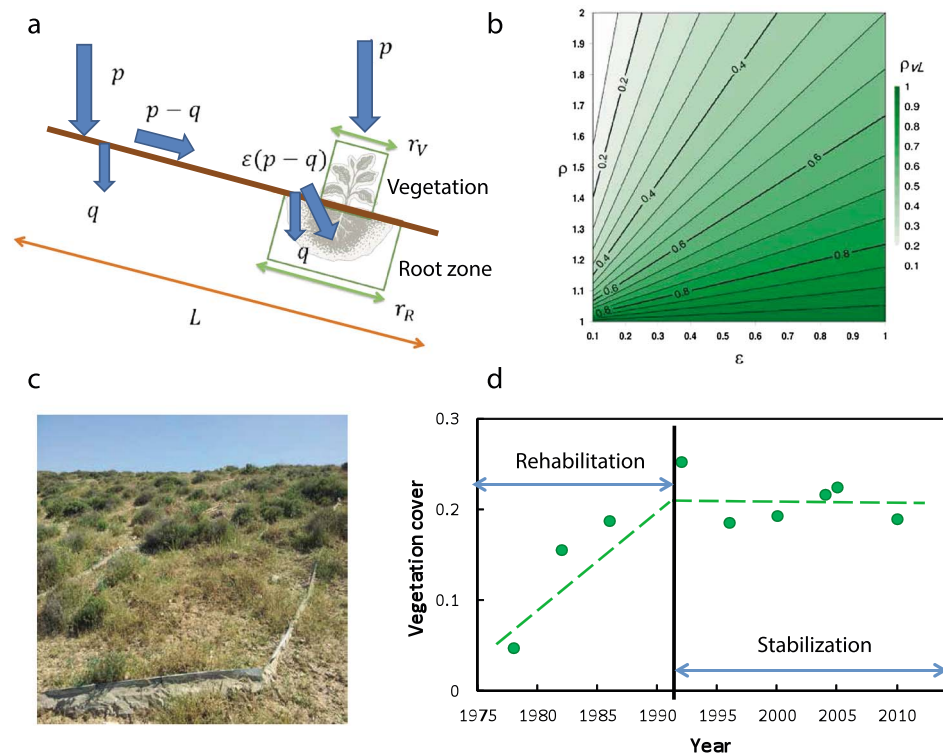


Figure 1. (a) The hillslope (length L) represented in the 1-D model. p and q represent the mean rainfall intensity and infiltration rates. $p-q$ is the overland flow produced when physical crusting causes $\kappa = q/p < 1$. ϵ is the fraction of overland flow entering the root zone. Plant available water is specified as ϕ , where $\phi = [1 + \kappa(p-1) + \epsilon(1-\kappa)(\rho_V^{-1}-1)]$. The vegetation density is quantified as $\rho_V = r_V/L$ and the lateral root extent as $\rho = r_R/r_V \geq 1$. (b) The fractional vegetation cover at which soil crusts reverse role from promoting to mitigating desertification, for plausible runoff capture efficiencies ($0.1 \leq \epsilon \leq 1$) and root-to-canopy ratios (ρ). (c) The experimental hillslope represented in the 2-D model (date: 17 April 2012). (d) Time evolution of the fractional vegetation cover, ρ_V , at the Lehavim LTER following grazing controls implemented in 1978. The plot shows a distinct rehabilitation period followed by stabilization of ρ_V .

Bare soil areas generated by loss of plant fractional cover can support the formation of physical and biological crusts. Physical soil crusts form either due to consolidation of soil material under rain impacts (structural crusts) or from the redistribution and accumulation of fine material (silica or salts) during surface runoff processes (depositional or erosion crusts) [Ries and Hirt, 2008]. Because physical crusts reduce infiltration capacity locally, they contribute to increasing runoff production during moderate to heavy rainfall events [Assouline, 2004; Assouline et al., 2007; Belnap, 2006; Fearnough et al., 1998; Savenije, 1995; Thompson et al., 2010]. In hot, arid drylands, biological soil crusts can have a similar effect, although in cooler deserts, biological crusts are also observed to enhance infiltration at the expense of surface runoff production [Belnap, 2006; Issa et al., 2011; Sole et al., 1997; Yair et al., 2011]. If runoff is unavailable to plants, then crusts reduce plant water availability and drive further desertification [Belnap, 2006; Cerdà, 1997; Kakembo et al., 2012; Kröpfl et al., 2013; Lavee et al., 1998; Palacio et al., 2014; Schlesinger et al., 1990]. If, however, the increased runoff is captured and infiltrates in vegetated sites or in regions accessed by laterally extensive plant root systems [Dunkerley and Brown, 1995; Eldridge et al., 2002; Galle et al., 1999; Li et al., 2008; Ludwig and Tongway, 1995; Ludwig et al., 1994; Valentin and d'Herbés, 1999; Valentin et al., 2001], then soil surface crusting can mitigate against desertification. Soil crust removal can lead to plant mortality in desert systems [Valentin and d'Herbés, 1999], while artificially induced biological crusts may support vegetation recovery [Lan et al., 2014]. There is, therefore, clear evidence of crusts both driving and mitigating against desertification. Throughout the analysis presented here, desertification is characterized in a simple fashion, based on a decline in plant fractional cover. Increases in plant fractional cover are taken to represent a recovering system.

Using a simplified budget for water movement on a uniform, partly vegetated slope subject to stationary hydrologic conditions, we explore the minimum necessary conditions that predict whether crusts drive or

mitigate desertification in the most idealized and generic conditions. To explore more realistic environmental conditions, a numerical model and field data from the Lehavim Long-Term Ecological Research (LTER) site in the semiarid area of the Negev, Israel, [Sela *et al.*, 2012; Yair and Kossovsky, 2002] are used. The Lehavim site offers a unique case study covering both land degradation and a subsequent 35 year recovery period. A combination of high-resolution monitoring of vegetation cover, in conjunction with detailed microtopographic, soil data, climate and hydrological measurements are available. Prior to 1977, the hillslopes at Lehavim were overgrazed and degraded. Following regulation of grazing in 1978, the fractional vegetation cover (ρ_v), as obtained from analysis of sub-1 m resolution aerial photography, recovered from 5–7% in 1978 to 20–25% in 1993 and has remained at 20–25% subsequently (Figure 1).

The role of crusts is shown to switch between promoting and ameliorating desertification, as a function of the local environmental conditions and vegetation fractional cover.

1.1. The LTER Case Study

The Lehavim Long-Term Ecological Research (LTER) site (31°20'N, 34°45'E) is located in the semiarid area of the northern Negev Desert, Israel, with an average rainfall of 290 mm per annum (the mean annual rainfall from 1978 to 2013, as measured by the Israel Meteorological Service, at the Lahav Station). The potential evapotranspiration (ET_p) during the growing season (October–May) is 770 mm. Of this total evaporative demand, only 600 mm of ET_p occurs after the first cumulative 5 mm of rainfall in the wet season (and thus has the potential to influence the runoff and water balance dynamics of the local vegetation). Lysimeter experiments on planted shrubs suggest that the vegetation water use during this period is approximately 0.8 ET_p [Sela *et al.*, 2015].

The Lehavim LTER is characterized by hilly terrain, emergent rock formations, and soils that are prone to physical crust formation. Today the site is sparsely vegetated (approximately 25% vegetation cover) with scattered dwarf shrubs (the dominant species is *Sarcopoterium spinosum*). Vegetation cover in the LTER has been highly dynamic over the past 35 years. Prior to 1978, the site was overgrazed, resulting in a very low fractional vegetation cover. In 1978, regulations on grazing were implemented, and the vegetation cover expanded. The site has been monitored throughout this period of vegetation recovery. To determine the drivers of this recovery and assess the role of soil crusting, we undertook an extensive site characterization that included a historical experimental runoff plot, which formed the basis for a two-dimensional modeling study. We analyzed air photos of the site during the vegetation recovery period to reconstruct the time sequence of recovery. Finally, we contextualized the dynamics at Lehavim by comparing the relation between vegetation fractional cover and plant water availability relative to rainfall inputs at other sparsely vegetated arid sites.

1.1.1. Site Characterization

The site characterization addressed topography, land cover, estimation of soil properties (with a focus on the water retention curve and the saturated hydraulic conductivity of both undisturbed and crusted soils), and estimation of seasonal vegetation water requirements. Topography was characterized over an **experimental runoff plot** (18.8 m × 4 m) [Chen *et al.*, 2013; Kossovsky, 1994], which also forms the focus of the 2-D modeling effort. Within this plot, elevation measurements were made on 0.5 m intervals ($n = 150$ measurements) with an electronic theodolite and interpolated using ordinary kriging (RMS error = 0.05 m) to produce a 5 cm horizontal resolution digital elevation model. Vegetation and rock cover within the site were mapped through analysis of aerial photos (see section 1.1.2).

The soils at the Lehavim LTER are brown lithosols and arid brown loess soils. Saturated hydraulic conductivity of undisturbed soil was estimated through infiltrometer measurements made below the canopy for every shrub in the infiltration plot [Sela *et al.*, 2012], giving $K_{sat} = 3 \text{ cm h}^{-1}$. Porosity was estimated using gravimetric methods. The water retention curve was obtained from a pedotransfer function parameterized for a Loess-type soil with a bulk density of 1.48 g cm^{-3} [Saxton *et al.*, 1986]. The undisturbed soil values only arise beneath the shrub canopy [Segoli *et al.*, 2008]. Beyond the canopy area, the bare soil surface is crusted. Crusts were found to be approximately uniform and to extend 2 cm into the soil [Sela *et al.*, 2012]. The hydraulic properties of the crust layer were estimated using the model of Mualem and Assouline [1989]. The crust saturated hydraulic conductivity was 2 orders of magnitude lower ($= 0.019 \text{ cm h}^{-1}$) than that of the undisturbed soil.

1.1.2. Air Photo Analysis

A historical air photo record provides an opportunity to characterize the spatial arrangement of emergent rock and shrubs on the site from 1978 to 2010. The historical photo record covers a $2 \times 2 \text{ km}^2$ area of north

facing hillslope with a resolution of <1 m. A supervised Maximum Likelihood Classification procedure [Svoray and Carmel, 2005] was used to delineate the image into rock-, soil-, shrub-, and grass-covered areas. The classification was validated against a visually classified set of 100 pixels per class and field observations. Fractional vegetation cover was estimated from the classified images as the total area of shrub canopy within each image. The resulting changes in vegetation cover at the LTER from 1978 to 2010 are depicted in Figure 1d. Three phases in the dynamics of the hillslope vegetation cover can be delineated: (1) overgrazing: with very low vegetation cover due to stress caused by high grazing pressure; (2) recovery: with recuperation following intensive plant growth due to initiation of grazing management; and (3) stabilization: with the stress of current grazing is in approximate equilibrium with plant growth, leading to a practically stable shrub cover around 20–25%. These classified images were then used as input to the 2-D modeling study in which the spatial arrangement of the vegetation and water flow paths are explicitly resolved. Vegetation cover for this modeling study was taken from an aerial image dated 4 September 1992, which coincided with the runoff measurements used to drive the 2-D model. Rock outcrops were mapped from a recent high-resolution ($10 \times 10 \text{ cm}^2$) orthophoto taken 31 December 2010.

1.1.3. Contextualization

To determine whether the dynamics in vegetation cover and plant water availability observed at Lehavim are generalizable, a literature search was conducted and identified three other arid sites with sufficient measurement of plant water use, infiltration, and runoff dynamics to allow comparison with the observed and modeled trends at Lehavim. The three sites were a banded vegetation site in the Sahel (Niger) [Galle *et al.*, 1999; Seghier and Galle, 1999]; the Meandu mine rehabilitation site in Queensland, Australia [Loch, 2000]; and the El Vento experimental catchment in Spain [Bautista *et al.*, 2007]. To obtain comparable data between the three sites and Lehavim, estimates were made of the plant available water and the annual water requirement of the vegetation. The techniques used varied depending on the data reported for each site. In Niger, two independent studies of the same region were used. In one study, Galle *et al.* [1999] measured infiltration volumes directly for 4 years. In a separate study conducted as part of the Hydrologic Atmospheric Pilot Experiment-Sahel campaign, transpiration was measured using the eddy covariance techniques (after adjusting for a minor soil evaporation) and was observed to comprise 70% of the cumulative volume of annual rainfall over the plot [Culf *et al.*, 1993]. In Queensland, Loch [2000] measured infiltration rates as a function of vegetation cover, and we used meteorological observations of the mean number of annual rain days and annual rainfall at the nearby weather station of Kingaroy to estimate mean rainfall volumes and intensities [Bureau of Meteorology, 2015]. The plant water requirement was estimated based on reported potential evaporation data and a measured crop coefficient for the dominant vegetation species, *Pennisetum clandestinum* [Nouri *et al.*, 2013]. In Spain, patch-scale runoff was measured directly in small plots at the El Vento experimental catchment [Bautista *et al.*, 2007]. The corresponding mean annual ET_p value is 1350 mm, and based on the peak rainfall period in the natural range of the dominant vegetation cover (*Stipa tenacissima*), and the plant water requirement was estimated to be approximately 400 mm/yr [Haase *et al.*, 1999].

2. Models

2.1. Simplified Theory: One-Dimensional Analytical Model

To determine whether soil crusts can play a dual role, switching between promoting and mitigating against desertification, a water balance was applied to a one-dimensional hillslope section, as shown in Figure 1. Surface runoff production Q per unit hill slope width is given by

$$Q = (p - q)(L - r_v) = (p - q)L\left(1 - \frac{r_v}{L}\right), \quad (1)$$

with the assumption that beneath the vegetated canopy, which is characterized by length scale r_v , infiltration rates are high enough that all incident rainfall infiltrates (and so no runoff is generated). The water infiltrating over the region defined by the root extent (r_r) is considered to represent the plant available water contribution for the storm. If the root zone is bounded by the plant canopy (i.e., $r_R \leq r_v$) and no runoff occurs, then the contributed plant available water is only that which infiltrates over r_v . Where $r_R > r_v$, the root zone receives additional water from bare soil infiltration over the region defined by $r_R - r_v$. Finally, if runoff occurs, then some fraction of the runoff ($=\varepsilon Q$) that enters the vegetated site may also infiltrate into the root zone. Here ε is the efficiency of runoff interception by the vegetated patches, where $\varepsilon = 1$ implies that all runoff is captured and $\varepsilon = 0$ implies no runoff is captured by vegetation at a given

hillslope position. In practice, ε varies with the slope, overland flow velocity, local hydraulic roughness from soil and vegetation, microtopography, soil hydraulic properties, antecedent soil moisture conditions across L , and the specific spatial arrangement of the vegetated patches downslope. For instance, a continuous band of vegetation growing along a contour might have $\varepsilon=1$, while a similar vegetated contour punctuated by bare soil would have $\varepsilon<1$. For the sake of the initial analysis, ε was treated as a control parameter that can be prescribed exogenously. Further, ε and other parameters were taken as being uniform across the hillslope, and independent of L . These assumptions are relaxed in 2-D modeling of the experimental plot shown in Figure 1c, as described in section 2.2.

The volume of water available for plant uptake is the total volume that infiltrates into the root zone per unit width of landscape F :

$$F = \varepsilon(p - q)(L - r_V) + q(r_R - r_V) + pr_V, \quad (2)$$

where the terms on the right-hand side represent the contribution of runoff from the bare sites to the vegetated sites, bare soil infiltration over the root zone extending beyond the canopy, and infiltration into the root zone beneath the vegetated canopy. Normalizing F by the rainfall amount and hillslope section length ($=pL$) results in

$$\frac{F}{pL} = V = \varepsilon(1 - \kappa)(1 - \rho_V) + \kappa(\rho_R - \rho_V) + \rho_V, \quad (3)$$

where $\rho_V = r_V/L$ is the fractional vegetation cover and $\rho_R = r_R/L$ is the fractional cover of the root zone. $\kappa = q/p$ is the infiltration capacity of bare soil normalized by rainfall intensity (<1 in the case of soil crusting). In the bare soil interspace, κ can vary from approximately 1, implying no physical crusting and minimal runoff, to <0.1 , representing the effects of a low-permeability soil crust that sheds most incident rainfall as runoff. The per storm inputs of plant available water at the hillslope scale are then normalized by the vegetation cover:

$$\phi = [1 + \kappa(\rho - 1) + \varepsilon(1 - \kappa)(\rho_V^{-1} - 1)]. \quad (4)$$

The metric ϕ is the main unit of analysis in the study, as it reflects the **incremental increase in the water resources available to support the growth of the standing vegetation per storm**. Equation (4) produces two limiting behaviors. The first is that in which the root extent is limited to the canopy radius ($\rho = 1$), and the vegetation is perfectly efficient in capturing runoff ($\varepsilon = 1$). In this case, the plant available water is described by

$$\phi = \kappa(1 - \rho_V^{-1}) + \rho_V^{-1}. \quad (5)$$

As $\kappa \rightarrow 0$, that is, as soil crusting renders bare sites increasingly impermeable, $\rho_V^{-1} \rightarrow 0$. Under these conditions, crusting *increases* plant water availability and does so most strongly for low fractional vegetation cover, creating a negative feedback between the extent of desertification, and water availability. The other limiting case assumes that runoff is not captured in vegetated sites (so $\varepsilon = 0$), while the root zone extends well beyond the canopy (e.g., $\rho = 2$ or more). In this case, the plant available water is given by

$$\phi = \kappa + 1. \quad (6)$$

In equation (6), increases in crusting (that is, decreases in κ) reduce water availability, independently of the fractional vegetation cover, and the presence of a crust layer is clearly deleterious. The differential sensitivity of ϕ to κ in equations (5) and (6) suggests one reason that the role of crusting has been controversial. This sensitivity can be **generalized by computing the rate of change in ϕ with respect to the relative infiltration capacity κ** . Soil crusting is a *driver* of desertification when $\partial\phi/\partial\kappa > 0$. Soil crusting *mitigates* against desertification when $\partial\phi/\partial\kappa < 0$. The transition between these cases (for fixed values of ε and ρ) occurs at a threshold vegetation cover ρ_{VL} when $\partial\phi/\partial\kappa = 0$:

$$\rho_{VL} = \varepsilon(\varepsilon + \rho - 1)^{-1}. \quad (7)$$

Provided $\rho_V < \rho_{VL}$, $\partial\phi/\partial\kappa < 0$, meaning that the soil crust is a positive factor that increases available water to vegetation and buffers against desertification potential.

The effects of variation in vegetation properties, $\partial\phi/\partial\rho$, are neglected in this analysis due to the separation between time scales of plant growth (weeks) and runoff generation (hours to days). The capture efficiency

ε was also treated as a static control parameter under the assumption that an effective ε value could be prescribed for any storm (even if capture efficiencies varied during the storm) and that while ε could be nonstationary (e.g., due to erosional or depositional processes within vegetation patches), these dynamics could not be a priori prescribed. Although crust morphology and its formation are not explicitly represented in the simple model, they are implicitly represented by the value of the infiltration capacity q over the duration of storm p .

As a second analysis, the potential magnitude of changes in plant water availability induced by the crusts was explored by computing $\phi(\kappa)$ for the vegetation cover corresponding to the range observed at the Lehavim LTER: $\rho_V = 0.07$ and 0.25 . Plant water availability is computed for low and high runoff capture efficiencies ($\varepsilon = 0.1$ and 0.9) and for three root-to-canopy zone ratios ($\rho = 1, 1.5$, and 2).

2.2. Two-Dimensional Numerical Model

The one-dimensional analysis highlights the importance of runoff capture efficiency as a determinant of the role of crusts. On any hillslope, the runoff capture efficiency, ε , during a storm event is a function of rainfall intensity, local slope, infiltration contrast between the vegetated and bare soil, and the spatial distribution of vegetation. These conditions determine the depth of ponding and the relative timescales of overland flow versus infiltration. The local microtopography determines the surface flow paths and the specific spatial arrangement of the vegetated patches with respect to both slope and microtopography, which then determines the likelihood that the vegetated patches intercept runoff.

These features were explored using a two-dimensional numerical model representing the experimental plots at the Lehavim LTER (Figure 1c). This model was calibrated and tested at the Lehavim LTER, where it predicted within-storm runoff depths to an accuracy of 15% [Chen *et al.*, 2013] (see details in the supporting information). In these model runs, the surface of the bare soil interspaces between vegetated patches is crusted. The specific κ value results from the measured hydraulic properties are applied to the crusted and uncrusted soil profiles. The κ values are estimated based on the crust model presented in Mualem and Assouline [1989]. Two values of fractional vegetation cover, 0.07 and 0.25 , corresponding to the limits of vegetation cover observed at the Lehavim LTER in the 1978–2013 period (Figure 1d), were explored. Two values of slope gradient, $s = 2\%$ and 35% , were used to represent the effective hillslope topography. The slope steepness was varied without altering the relative relief associated with microtopography, so the relative elevation of microtopographic variations with respect to overland flow were preserved between the model runs. For each combination of vegetation cover and slope, an average seasonal rain volume (corresponding to the 1978–2013 mean seasonal rainfall of 300 mm) was applied to the hillslope using different mean storm intensity values p , ranging from 5 to 25 mm/h. The ratio of plant available water to the seasonal plant water requirement was computed, using the assumption that $\rho = 1$. The mean annual plant water requirement at the Lehavim LTER was estimated to be 80% of the seasonal potential evaporation of 600 mm, as presented above. The model output is equivalent to normalizing the metric ϕ by ϕ^* , where ϕ^* represents the plant water requirement per unit of rainfall depth and vegetated area. Thus, the one-dimensional and two-dimensional model results can be related to each other.

A final analysis used the two-dimensional model to interrogate the role of soil crusting at the Lehavim vegetation recovery from degradation observed from 1978 to 2010 (Figure 1d). The modeling of plant water availability was carried out for a measured mean hillslope of 16% using the specific rainfall measurements corresponding to each year during that period. Vegetation cover was varied to reflect observations in air photos. The model runs were performed with two contrasting soil conditions—with and without soil crusts, to isolate the effects of crusting on the trajectory of recovery as represented in the model. The results were contextualized by comparison with the data from the three other arid sites, located in Australia, Niger, and Spain, and which are characterized by sparse vegetation cover and physical crust formation on bare soil areas.

3. Results

3.1. One-Dimensional Analytical Model

The vegetation cover conditions for which the role of soil surface crusting switches from driving to mitigating desertification are given by the solution of equation (7). Figure 1b presents contour lines of the threshold vegetation cover ρ_{VL} determined over a plausible range of runoff capture efficiencies ($0.1 < \varepsilon < 1$) and

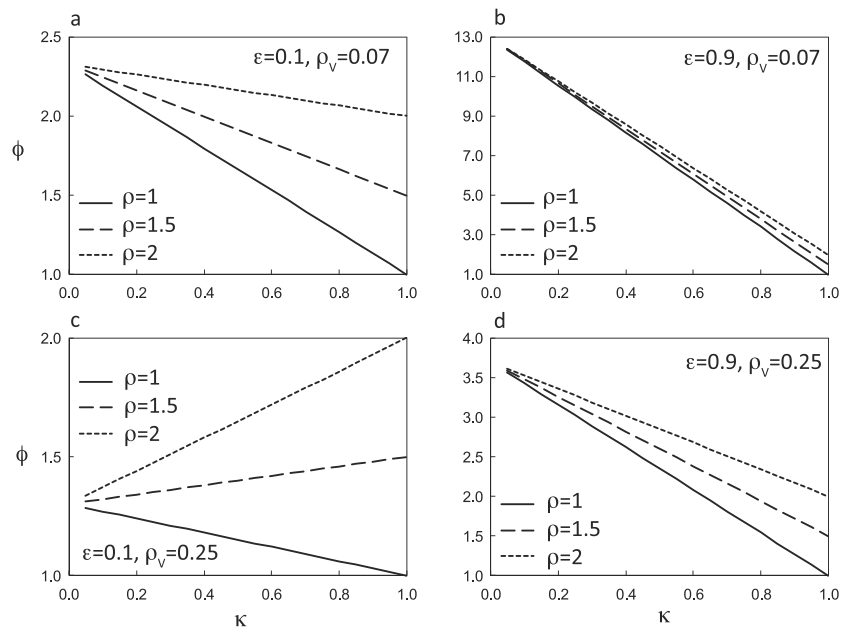


Figure 2. The enhancement of plant water availability relative to rainfall input as a function of the degree of surface crusting $\phi(k)$ based on equation (4). Four cases, representing combinations of high and low runoff capture efficiencies by the vegetation patches ($\epsilon = 0.9$) and low ($\rho = 0.1$) and high and low vegetation cover (set to the limits of ρ_V observed at the Lehavim LTER, 0.07 and 0.25) are explored, with three representative root canopy morphologies shown in each case. (a) A low capture efficiency and low vegetation cover, (b) a high capture efficiency and low vegetation cover, (c) a low capture efficiency and the Lehavim equilibrium vegetation cover, and (d) a high capture efficiency with the equilibrium Lehavim vegetation cover.

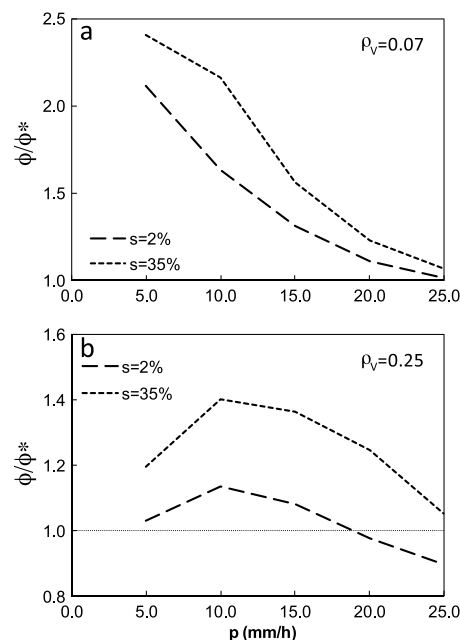


Figure 3. The variation of the ratio of plant available water to plant water demand (on seasonal scales) with changing mean storm intensity p , $\frac{\phi}{\phi^*}(p)$, for shallow ($s = 2\%$) and steep ($s = 35\%$) slopes, and for (a) sparse ($\rho_V = 0.07$) and (b) intermediate ($\rho_V = 0.25$) vegetation representing the limits of ρ_V observed at the Lehavim LTER.

root-to-canopy zone ratios ($1 < \rho < 2$). The region above a given ρ_{VL} contour line represents the range of environmental conditions for a particular value of ρ_V under which crusts *amplify* desertification. The region below that contour line represents environmental conditions under which soil crusting mitigates against desertification. For high fractional vegetation cover, soil crusts *amplify* desertification for almost all environmental conditions. For intermediate vegetation cover, soil crusting *amplifies* desertification if vegetation patches cannot access runoff water ($\epsilon \ll 1$) or if the plant water uptake is governed by a large lateral extension of the root zone beyond the canopy ($\rho \gg 1$). Otherwise, crusting mitigates against desertification for intermediate vegetation cover. For low vegetation cover, soil crusting mitigates against desertification for almost all hydrologic conditions. Thus, depending on the environmental context in which soil crusts occur, they may either increase or reduce vegetation water availability, and either promote or buffer against desertification.

The magnitude of the effects of soil crusting on plant available water is illustrated for four contrasting cases in Figure 2. The plots show a trade-off between crusting, runoff capture, and lateral root extension as mechanisms that govern plants access to water. Where runoff capture is inefficient, the value of increasing the rooting extent declines directly with increased crust formation (decreasing κ), regardless of the vegetation cover (Figures 2a and 2d). If runoff capture efficiency is high, the inputs of plant available water are

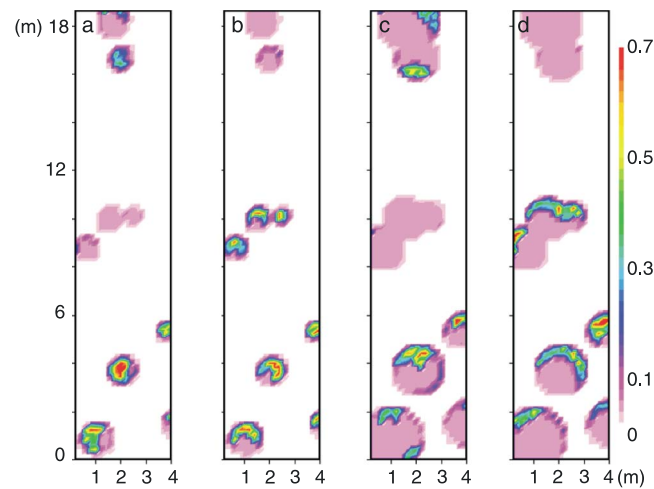


Figure 4. Modeled cumulative infiltration on vegetation patches for (a and c) shallow and (b and d) steep slopes, preserving local microtopographic relief. Figures 4a and 4b represent the low vegetation cover case ($\rho_v = 0.07$), while Figures 4c and 4d represent the equilibrium vegetation cover at Lehavim, ($\rho_v = 0.25$). Cumulative infiltration depths shown are in meters. Although steeper slopes increase runoff velocities (and thus reduce the efficiency of runoff capture near the top of the slope), the greater runoff production on steeper slopes prevents runoff from being routed away from the midslope vegetated patches by a microtopographic rise, increasing the overall efficiency of vegetation patch interception and infiltration.

desertification at Lehavim LTER, by ensuring that plant available water inputs exceeded not only rainfall but also the plant water requirement (i.e., $\phi/\phi^* > 1$) for almost all cases tested (Figure 3). For low vegetation cover, the crusts lead to $\phi/\phi^* > 1$ for all slope and rainfall intensity combinations, approaching $\phi/\phi^* = 1$ as the rainfall intensity increased. This decline in plant water availability with rainfall intensity can be interpreted as a reduction in the efficiency of water capture by the low vegetation cover as runoff flow velocities increase (Figure 3a). By contrast, for higher vegetation cover, a peak value of ϕ/ϕ^* was obtained at intermediate rainfall intensities (Figure 3b). In both cases, steeper slopes increased plant available water due to an increase in vegetation patch capture efficiency. This increase in capture efficiency with slope arose due to the interaction between microtopography and vegetation patch positioning (Figure 4). Steeper slopes logically increase runoff production and decrease infiltration over the vegetation patches near the top of the hillslope. However, this increase is compensated for by increased runoff capture in the midsection of the hillslope. In the midsection, local microtopographic rises diverted water from the vegetation patches where the mean slope was low but did not divert water under deeper, faster flow conditions.

Figure 5a illustrates the effect of recovery from degradation at Lehavim on plant-modeled available water. For low vegetation cover, the plant water availability exceeds the plant water demand ($\phi/\phi^* > 1$), but the ratio of water availability to water demand declines as the vegetation cover increases, reaching equivalence $\phi/\phi^* = 1$ for vegetation cover of 25%, approximately the equilibrium vegetation cover observed at Lehavim [Svoray et al., 2008]. Repeating the model runs in the absence of soil surface crusting in the bare area resulted in $\phi/\phi^* = 0.5$.

Figure 5b illustrates the trends at Lehavim LTER in the context of similar relations between vegetation cover and plant available water at three other arid sites. Based on the reported measurements on fractional vegetation cover, ρ_v , and water balance components, the respective ϕ/ϕ^* values for each site were estimated. In the Sahel, direct observations of rainfall, infiltration, and transpiration rates led to $\phi/\phi^* = (2.77/2.35) = 1.18$. In Queensland, measured infiltration rates as a function of vegetation cover and meteorological observations allowed estimates of κ . Assuming that $\varepsilon = 1$, we computed ϕ for each fractional vegetation cover from equation (4). The plant water requirement was estimated based on reported potential evaporation data and a measured crop coefficient for the dominant vegetation species, *Pennisetum clandestinum*, leading to $\phi^* = 1.035$. In Spain, patch-scale runoff data and measured fractional vegetation cover enabled a direct estimate of ϕ for each patch, assuming $\varepsilon = 1$, and using equation (1). Based on the peak rainfall in the

insensitive to root morphology for low vegetation cover (Figure 2b). For sufficiently high runoff production (i.e., for low κ), the inputs of plant available water per storm may be as large as $\phi > 10$, comparable to observations of infiltration enhancements reported by Galle et al. [1999] in Niger ($\phi \sim 8$). If vegetation cover is high, but the efficiency of vegetated sites in capturing runoff is low (Figure 2c), then plant available water cannot be enhanced relative to rainfall input ($\phi \leq 2$) and crusts mitigate against desertification only for plants with $\rho = 1$. If $\rho > 1$, crusting promotes desertification in all cases, with the most extreme reductions in ϕ being on the order of 35%.

3.2. Two-Dimensional Numerical Model

Consistent with the predictions of the one-dimensional model, the presence of soil surface crusting mitigated against

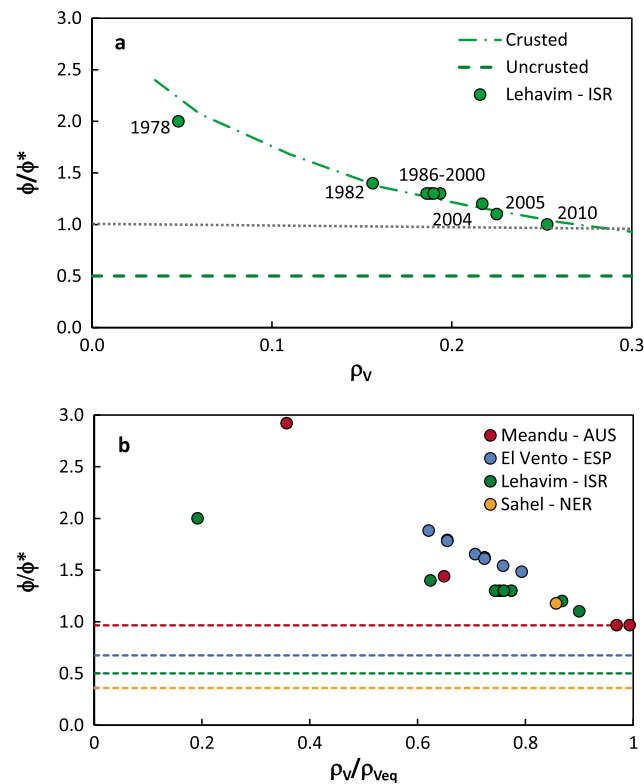


Figure 5. (a) The modeled relation between (ϕ/ϕ^*) and ρ_V for the LTER in the case of a sealed (dashed green curve) or unsealed bare soil areas (dashed black line). The $\phi/\phi^* = 1$ line indicates that seasonal cumulative infiltration meets the plant water need. Green dots represent the observed vegetation cover at the Lehavim LTER from 1978 to 2008. (b) Intersite comparison of the dependence between vegetation cover ρ_V and plant water availability (ϕ/ϕ^*) for the Lehavim LTER, Meandu Mine Rehabilitation site (Queensland, Australia [Loch, 2000]), the El Vento Experimental Catchment (Spain [Bautista et al., 2007]), and a region of banded vegetation in the Sahel (Niger [Galle et al., 1999]). Vegetation cover is shown relative to the peak (equilibrium) vegetation cover at each site (ρ_V/ρ_{Veq}).

switched from driving desertification in cases of high vegetation cover to mitigating desertification as vegetation cover declined. Desertification induced by crusts may thus be self-limiting. If other pressures on dryland vegetation are alleviated, crust formation may support reestablishment of vegetation as occurred at the Lehavim LTER during the 1978–2008 period (Figure 1d).

The two-dimensional model results have several implications. First, runoff-runon generation arose on shallow slopes, consistent with prior simulations for flat terrain where infiltration excess runoff flow is driven by a permeability contrast between soil and vegetated sites [Thompson et al., 2011]. Second, although the “switching” of crusts from mitigating desertification to promoting desertification was not observed in the model runs made at the Lehavim LTER, the trends in plant water availability with vegetation cover were consistent with predictions from the one-dimensional model. Crusts were less effective at buffering against desertification as vegetation cover increased. Higher rainfall intensity (lower κ) and lower slopes (decreasing ε at this site due to the interaction between microtopography and runoff) reduced the ability of crusts to buffer desertification.

Without crusting, runoff did not supply additional water to vegetation. In these cases, seasonal infiltration was lower than plant water needs. This suggests that in the absence of soil crusts, the current vegetation cover in most of the sites considered would be unstable (this is probably not accurate for the site at Queensland), and the site trajectories would be toward lower vegetation cover and potentially desertification.

natural range of the dominant vegetation cover (*Stipa tenacissima*), approximately 400 mm/yr, ϕ^* was estimated to be equal to 1.48.

To compare the four sites characterized by different soils, vegetation types, and climatic conditions, the local ρ_V values were normalized using the estimated vegetation cover at equilibrium (i.e., for conditions where $\phi/\phi^* = 1$), ρ_{Veq} , specific for each location. For the Sahel site, an average value of 35% was taken reflecting the lower and upper limits of reported values described elsewhere [Culf et al., 1993; Galle et al., 1999]. For the Meandu site (Queensland) and the Lehavim LTER (Israel), reported maximal data values of 42% and 25%, respectively, were used. For the El Vento site (Spain), a value of 58% was estimated based on extrapolating the $(\rho_V, \phi/\phi^*)$ curve fitted to the data and the intersection with the $\phi/\phi^* = 1$ line.

As shown in Figure 5b, similar trends in ϕ/ϕ^* as a function of vegetation cover are found for Lehavim and the three other arid sites considered. Crusting is apparently necessary to support vegetation at all sites ($\phi/\phi^* < 1$ in the absence of crusting). Vegetation cover appears to saturate at site-specific equilibrium values (ρ_{Veq}) in the limit of $\phi/\phi^* = 1$.

4. Discussion

Both one- and two-dimensional models indicate that the role of physical crusts

The analytical and site-specific 2-D numerical model results indicate that soil surface crusting has a dual role in desertification. Physical crusts (and, in hot deserts, biological crusts) that reduce infiltration tend to accelerate desertification when (i) vegetation cover is relatively dense, (ii) plants are dependent on infiltration in bare soil sites (root zone expanding beyond from the canopy area), and (iii) vegetated patches have limited ability to intercept and infiltrate runoff. Conversely, crusts mitigate desertification if runoff infiltrates in vegetated sites, vegetation cover is sparse, and the root zone is largely confined to the canopy area. The efficiency of runoff capture by vegetated plots is driven by a combination of rainfall intensity, vegetation spatial arrangement and its correlation with microtopography, and the mean slope, which are difficult to prescribe a priori without detailed site-specific measurements. However, for a fixed set of hillslope conditions, crusts can reverse their role as a function of vegetation cover, indicating that desertification induced by crusting can be self-limiting—or conversely, that vegetation recovery assisted by crust formation will also lead to a stable plant fractional cover, as observed at the Lehavim LTER. At Lehavim, desertification was induced by overgrazing, which reduced the vegetation cover [Schlesinger *et al.*, 1990], increasing the relative area of bare soil surfaces prone to crusting. When the grazing pressure was alleviated, the increase in water availability resulting from the relatively large portion of crusted areas induced a rehabilitation process, so the vegetation cover increased to a quasi-stable level representing an equilibrium with the local environmental conditions.

These findings neglect a detailed consideration of other factors that drive desertification and their interaction with crust formation. In practice, soil crusts, whether biological or physical, interact with other desertification drivers including aeolian and water erosion, plant dispersal and establishment, or biogeochemical cycling. However, crust formation tends to retard wind erosion, increasing the capture of atmospherically deposited dust and associated nutrients [Belnap, 2003]. On the other hand, crust formation is frequently associated with increased risk of rill formation due to the enhancement of runoff production and erosive velocities [Valentin *et al.*, 2005]. The formation of rills, moreover, corresponds to a concentrated overland flow path in which water is less likely to be effectively intercepted and reinfilted by vegetated sites, reducing the efficiency metric ε and increasing the risk of desertification. Although recovery of vegetation on crusted sites is clearly possible, as illustrated by both the Lehavim case study and by successful use of synthetic crusts to reestablish vascular plants [Lan *et al.*, 2014], there are also reports of seed establishment being retarded on crusted soils [Prasse and Bornkamm, 2000; Zaady *et al.*, 1997]. As advances in cyanobacterial inoculation technology now allow for rapid (3–8 years) formation of engineered biological crusts [Lan *et al.*, 2014], the selective deployment of these techniques in regions where crusts can support vegetation growth and mitigate desertification rather than enhancing desertification will be important. While the analysis here indicates the “generic” conditions under which crusts are beneficial, it also highlights that site-specific interaction of microtopography, rainfall characteristics, vegetation distributions, and slopes should be examined to evaluate the impact of soil crusts on desertification risk.

5. Conclusion

Studies exploring desertification and arid land degradation record divergent perspectives on the functional role of bare soil sites—as either amplifying or retarding degradation processes. Focusing on the ecohydrological role of these sites, we have demonstrated that soil surface sealing and runoff generation can induce both positive and negative feedbacks to plant available water in a dryland system, depending on the physiological adaptations exhibited by vegetation, the interplay of runoff with local microtopography and slopes and the efficiency with which vegetated patches intercept and retain runoff. A nuanced interpretation of how crusting and bare sites interact with surface runoff processes would enable targeted land management and restoration options to target mitigation of any negative consequences of bare sites, or, conversely, enhancement of positive feedback mechanisms by which bare sites and soil crusting increase plant available water above those determined solely by rainfall.

Acknowledgments

This research was partly supported by the Israel Science Foundation (ISF) (grant 564 1184/11) and by the International Arid Lands Consortium (grant 10R–09). This support is gratefully acknowledged. The data used in this study are available upon request.

References

- Álvarez-Martínez, J., A. Gómez-Villar, and T. Lasanta (2013), The use of goats grazing to restore pastures invaded by shrubs and avoid desertification: A preliminary study in the Spanish Cantabrian Mountains, *Land Degrad. Dev.*, doi:10.1002/ldr.2230.
- Assouline, S. (2004), Rainfall-induced soil surface sealing, *Vadose Zone J.*, 3(2), 570–591, doi:10.2113/3.2.570.
- Assouline, S., J. Selker, and J.-Y. Parlange (2007), A simple accurate method to predict time of ponding under variable intensity rainfall, *Water Resour. Res.*, 43, W03426, doi:10.1029/2006WR005138.

- Barbero-Sierra, C., M. J. Marques, M. Ruiz-Pérez, R. Escadafal, and W. Exbrayat (2015), How is desertification research addressed in Spain?, *Land Versus Soil Approaches*, 26(5), 423–432, doi:10.1002/ldr.2344.
- Bautista, S., A. G. Mayor, J. Bourakhouadar, and J. Bellot (2007), Plant spatial pattern predicts hillslope runoff and erosion in a semiarid Mediterranean landscape, *Ecosystems*, 10(6), 987–998, doi:10.1007/s10021-007-9074-3.
- Belnap, J. (2003), Biological soil crusts and wind erosion, in *Biological Soil Crusts: Structure, Function, and Management*, edited by J. Belnap and O. Lange, pp. 339–347, Springer, Berlin, doi:10.1007/978-3-642-56475-8_25.
- Belnap, J. (2006), The potential roles of biological soil crusts in dryland hydrologic cycles, *Hydrol. Processes*, 20(15), 3159–3178, doi:10.1002/hyp.6325.
- Bisaro, A., M. Kirk, P. Zdruli, and W. Zimmermann (2014), Global drivers setting desertification research priorities: Insights from a stakeholder consultation forum, *Land Degrad. Dev.*, 25(1), 5–16, doi:10.1002/ldr.2220.
- Brandt, M., C. Mbow, A. A. Diouf, A. Verger, C. Samimi, and R. Fensholt (2015), Ground- and satellite-based evidence of the biophysical mechanisms behind the greening Sahel, *Global Change Biol.*, 21(4), 1610–1620, doi:10.1111/gcb.12807.
- Bureau of Meteorology (2015), *Map of Climatic Averages*, Government of Australia.
- Cerdà, A. (1997), The effect of patchy distribution of *Stipa tenacissima* L. on runoff and erosion, *J. Arid Environ.*, 36(1), 37–51, doi:10.1006/jare.1995.0198.
- Chen, L., S. Sela, T. Svoray, and S. Assouline (2013), The role of soil-surface sealing, microtopography, and vegetation patches in rainfall-runoff processes in semiarid areas, *Water Resour. Res.*, 49(9), 5585–5599, doi:10.1002/wrcr.20360.
- Culff, A. D., S. J. Allen, J. H. C. Gash, C. R. Lloyd, and J. S. Wallace (1993), Energy and water budgets of an area of patterned woodland in the Sahel, *Agric. For. Meteorol.*, 66(1–2), 65–80, doi:10.1016/0168-1923(93)90082-5.
- Dardel, C., L. Kergoat, P. Hiernaux, E. Mougin, M. Grippa, and C. Tucker (2014), Re-greening Sahel: 30years of remote sensing data and field observations (Mali, Niger), *Remote Sens. Environ.*, 140, 350–364.
- Deblauwe, V., N. Barbier, P. Couteron, O. Lejeune, and J. Bogaert (2008), The global biogeography of semi-arid periodic vegetation patterns, *Global Ecol. Biogeogr.*, 17(6), 715–723, doi:10.1111/j.1466-8238.2008.00413.x.
- D'Odorico, P., A. Bhattachan, K. F. Davis, S. Ravi, and C. W. Runyan (2013), Global desertification: Drivers and feedbacks, *Adv. Water Resour.*, 51, 326–344, doi:10.1016/j.advwatres.2012.01.013.
- Dunkerley, D., and K. Brown (1995), Runoff and runoff areas in patterned chenopod shrubland, arid western New South Wales, Australia: Characteristics and origin, *J. Arid Environ.*, 30(1), 41–55, doi:10.1016/S0140-1963(95)80037-9.
- Eldridge, D., E. Zaady, and M. Shachak (2002), Microphytic crusts, shrub patches and water harvesting in the Negev Desert: The Shikim system, *Landscape Ecol.*, 17(6), 587–597, doi:10.1023/a:1021575503284.
- Fearnough, W., M. Fullen, D. Mitchell, I. Trueman, and J. Zhang (1998), Aeolian deposition and its effect on soil and vegetation changes on stabilised desert dunes in northern China, *Geomorphology*, 23(2), 171–182, doi:10.1016/S0169-555X(97)00111-6.
- Flecken, L., and L. C. Stringer (2014), Land management and policy responses to mitigate desertification and land degradation, *Land Degrad. Dev.*, 25(1), 1–4, doi:10.1002/ldr.2272.
- Galle, S., M. Ehrmann, and C. Peugeot (1999), Water balance in a banded vegetation pattern: A case study of tiger bush in western Niger, *Catena*, 37(1), 197–216, doi:10.1016/S0341-8162(98)90060-1.
- Haase, P., F. Pugnaire, S. C. Clark, and L. D. Incoll (1999), Environmental control of canopy dynamics and photosynthetic rate in the evergreen tussock grass *Stipa tenacissima*, *Plant Ecol.*, 145(2), 327–339, doi:10.1023/a:1009892204336.
- Issa, O. M., C. Valentin, J.-L. Rajot, O. Cerdan, J.-F. Desprats, and T. Bouchet (2011), Runoff generation fostered by physical and biological crusts in semi-arid sandy soils, *Geoderma*, 167, 22–29, doi:10.1016/j.geoderma.2011.09.013.
- Kakembo, V., S. Ndlela, and E. Cammeraat (2012), Trends in vegetation patchiness loss and implications for landscape function: The case of *Pteronia incana* invasion in the Eastern Cape Province, South Africa, *Land Degrad. Dev.*, 23(6), 548–556, doi:10.1002/ldr.2175.
- Kossovsky, A. (1994), Generation of runoff in first order drainage basins in a semi-arid region, Lahav Hills, Negev, Israel MSc thesis, 124 pp., The Hebrew Univ., Jerusalem.
- Kröpfl, A. I., G. A. Cecchi, N. M. Villaluso, and R. A. Distel (2013), Degradation and recovery processes in patchy rangelands of Northern Patagonia, Argentina, *Land Degrad. Dev.*, 24(4), 393–399, doi:10.1002/ldr.1145.
- Lan, S., Q. Zhang, L. Wu, Y. Liu, D. Zhang, and C. Hu (2014), Artificially accelerating the reversal of desertification: Cyanobacterial inoculation facilitates the succession of vegetation communities, *Environ. Sci. Technol.*, 48(1), 307–315, doi:10.1021/es403785j.
- Lavee, H., A. Imeson, and P. Sarah (1998), The impact of climate change on geomorphology and desertification along a Mediterranean-arid transect, *Land Degrad. Dev.*, 9(5), 407–422, doi:10.1002/(SICI)1099-145X(199809/10)9:5<30.CO;2-6.
- Li, X. J., X. R. Li, W. M. Song, Y. P. Gao, J. G. Zheng, and R. L. Jia (2008), Effects of crust and shrub patches on runoff, sedimentation, and related nutrient (C, N) redistribution in the desertified steppe zone of the Tengger Desert, Northern China, *Geomorphology*, 96(1–2), 221–232, doi:10.1016/j.geomorph.2007.08.006.
- Loch, R. J. (2000), Effects of vegetation cover on runoff and erosion under simulated rain and overland flow on a rehabilitated site on the Meandu Mine, Tarong, Queensland, *Aust. J. Soil Res.*, 38(2), 299–312, doi:10.1071/SR99030.
- Ludwig, J. A., and D. J. Tongway (1995), Spatial organisation of landscapes and its function in semi-arid woodlands, Australia, *Landscape Ecol.*, 10(1), 51–63, doi:10.1007/BF00158553.
- Ludwig, J. A., D. J. Tongway, and S. G. Marsden (1994), A flow-filter model for simulating the conservation of limited resources in spatially heterogeneous, semi-arid landscapes, *Pac. Conserv. Biol.*, 1(3), 209–213, doi:10.1071/PC940209.
- Miao, L., J. C. Moore, F. Zeng, J. Lei, J. Ding, B. He, and X. Cui (2015), Footprint of research in desertification management in China, *Land Degrad. Dev.*, doi:10.1002/ldr.239.
- Millennium Ecosystem Assessment (2003), *Ecosystems and Human Well-Being: A Framework for Assessment*, Millennium Ecosyst. Assess. Ser., Island Press, Washington, D. C.
- Mualem, Y., and S. Assouline (1989), Modeling soil seal as a nonuniform layer, *Water Resour. Res.*, 25(10), 2101–2108, doi:10.1029/WR025i010p02101.
- Nouri, H., S. Beecham, A. M. Hassanli, and F. Kazemi (2013), Water requirements of urban landscape plants: A comparison of three factor-based approaches, *Ecol. Eng.*, 57, 276–284, doi:10.1016/j.ecoleng.2013.04.025.
- Olsson, L., L. Eklundh, and J. Ardo (2005), A recent greening of the Sahel—Trends, patterns and potential causes, *J. Arid Environ.*, 63(3), 556–566.
- Palacio, R. G., A. J. Bisigato, and P. J. Bouza (2014), Soil erosion in three grazed plant communities in Northern Patagonia, *Land Degrad. Dev.*, 25(6), 594–603, doi:10.1002/ldr.2289.
- Prasse, R., and R. Bornkamm (2000), Effect of microbiotic soil surface crusts on emergence of vascular plants, *Plant Ecol.*, 150(1–2), 65–75, doi:10.1023/A:1026593429455.
- Reynolds, J. F., D. M. S. Smith, E. F. Lambin, B. Turner, M. Mortimore, S. P. Batterbury, T. E. Downing, H. Dowlatabadi, R. J. Fernandez, and J. E. Herrick (2007), Global desertification: Building a science for dryland development, *Science*, 316(5826), 847–851, doi:10.1126/science.1131634.

- Ries, J. B., and U. Hirt (2008), Permanence of soil surface crusts on abandoned farmland in the Central Ebro Basin/Spain, *Catena*, 72(2), 282–296, doi:10.1016/j.catena.2007.06.001.
- Salvati, L., M. Zitti, and L. Perini (2013), Fifty years on: Long-term patterns of land sensitivity to desertification in Italy, *Land Degrad. Dev.*, doi:10.1002/ldr.2226.
- Savenije, H. (1995), Does moisture feedback affect rainfall significantly?, *Phys. Chem. Earth*, 20(5–6), 507–513, doi:10.1016/S0079-1946(96)00014-6.
- Saxton, K., W. J. Rawls, J. Romberger, and R. Papendick (1986), Estimating generalized soil-water characteristics from texture, *Soil Sci. Soc. Am. J.*, 50(4), 1031–1036, doi:10.2136/sssaj1986.03615995005000040039x.
- Scheffer, M., S. Carpenter, J. A. Foley, C. Folke, and B. Walker (2001), Catastrophic shifts in ecosystems, *Nature*, 413(6856), 591–596, doi:10.1038/35098000.
- Schlesinger, W. H., J. Reynolds, G. L. Cunningham, L. Huenneke, W. Jarrell, R. Virginia, and W. Whitford (1990), Biological feedbacks in global desertification, *Science*, 247(4946), 1043–1048, doi:10.1126/science.247.4946.1043.
- Seghier, J., and S. Galle (1999), Run-on contribution to a Sahelian two-phase mosaic system: Soil water regime and vegetation life cycles, *Acta Oecol.*, 20(3), 209–217, doi:10.1016/S1146-609X(99)80033-2.
- Segoli, M., E. D. Ungar, and M. Shachak (2008), Shrubs enhance resilience of a semi-arid ecosystem by engineering and regrowth, *Ecology*, 89(4), 330–339, doi:10.1002/eco.21.
- Sela, S., T. Svoray, and S. Assouline (2012), Soil water content variability at the hillslope scale: Impact of surface sealing, *Water Resour. Res.*, 48, W03522, doi:10.1029/2011WR011297.
- Sela, S., T. Svoray, and S. Assouline (2015), The effect of soil surface sealing on vegetation water uptake along a dry climatic gradient, *Water Resour. Res.*, doi:10.1002/2015WR017109.
- Sole, A., A. Calvo, A. Cerda, R. La, R. Pini, and J. Barbero (1997), Influences of micro-relief patterns and plant cover on runoff related processes in badlands from Tabernas (SE Spain), *Catena*, 31(1), 23–38.
- Svoray, T., and Y. Carmel (2005), Empirical method for topographic correction in aerial photographs, *IEEE Geosci. Remote Sens. Lett.*, 2(2), 211–214, doi:10.1109/LGRS.2005.846012.
- Svoray, T., R. Shafran-Nathan, Z. Henkin, and A. Perevolotsky (2008), Spatially and temporally explicit modeling of conditions for primary production of annuals in dry environments, *Ecol. Modell.*, 218(3), 339–353, doi:10.1016/j.ecolmodel.2008.07.029.
- Thompson, S., C. J. Harman, P. Heine, and G. G. Katul (2010), Vegetation-infiltration relationships across climatic and soil type gradients, *J. Geophys. Res.*, 115, G02023, doi:10.1029/2009JG001134.
- Thompson, S., G. Katul, A. Konings, and L. Ridolfi (2011), Unsteady overland flow on flat surfaces induced by spatial permeability contrasts, *Adv. Water Resour.*, 34(8), 1049–1058, doi:10.1016/j.advwatres.2011.05.012.
- Torres, L., E. M. Abraham, C. Rubio, C. Barbero, and M. Ruiz (2015), Desertification research in Argentina, *Land Degrad. Dev.*, doi:10.1002/ldr.2392.
- United Nations Convention to Combat Desertification (UNCCD) (2012), *Zero Net Land Degradation, a Sustainable Development Goal for Rio 20+ to Secure the Contribution of Our Planet's Land and Soil to Sustainable Development, Including Food Security and Poverty Eradication*, 17 pp., UNCCD secretariat, Bonn, Germany.
- United Nations (1994), United Nations convention to combat desertification, elaboration of an international convention to combat desertification in countries experiencing serious drought and/or desertification, particularly in Africa Rep., United Nations.
- Valentin, C., and J.-M. d'Herbès (1999), Niger tiger bush as a natural water harvesting system, *Catena*, 37(1), 231–256, doi:10.1016/S0341-8162(98)00061-7.
- Valentin, C., D. J. Tongway, and J. Seghier (2001), Banded landscapes: Ecological developments and management consequences, in *Banded Vegetation Patterning in Arid and Semiarid Environments*, *Ecol. Stud.*, vol. 149, edited by D. J. Tongway, C. Valentin, and J. Seghier, pp. 228–243, Springer, New York, doi:10.1007/978-1-4613-0207-0_12.
- Valentin, C., J. Poesen, and Y. Li (2005), Gully erosion: Impacts, factors and control, *Catena*, 63(2–3), 132–153, doi:10.1016/j.catena.2005.06.001.
- Vicente-Serrano, S. M., A. Zouber, T. Lasanta, and Y. Pueyo (2012), Dryness is accelerating degradation of vulnerable shrublands in semiarid Mediterranean environments, *Ecol. Monogr.*, 82(4), 407–428, doi:10.1890/11-2164.1.
- Wang, T., C. Yan, X. Song, and S. Li (2013), Landsat images reveal trends in the aeolian desertification in a source area for sand and dust storms in China's Alashan Plateau (1975–2007), *Land Degrad. Dev.*, 24(5), 422–429.
- Yair, A., and A. Kossovsky (2002), Climate and surface properties: Hydrological response of small arid and semi-arid watersheds, *Geomorphology*, 42(1), 43–57, doi:10.1016/S0169-555X(01)00072-1.
- Yair, A., R. Almog, and M. Veste (2011), Differential hydrological response of biological topsoil crusts along a rainfall gradient in a sandy arid area: Northern Negev Desert, Israel, *Catena*, 87(3), 326–333, doi:10.1016/j.catena.2011.06.015.
- Zaady, E., Y. Gutterman, and B. Boeken (1997), The germination of mucilaginous seeds of *Plantago coronopus*, *Reboudia pinnata*, and *Carrichtera annua* on cyanobacterial soil crust from the Negev Desert, *Plant Soil*, 190(2), 247–252, doi:10.1023/A:1004269031844.